Research of Stress Rearrangement in a Crack After Repeatable Elasto-plastic Tension

Vengrinovich V.L., Denkevich Yu.B. and Gerlovsky S.A.
Institute of Applied Physics of the National Academy of Sciences of Belarus

Abstract

The effect of repeated elasto-plastic deformation by tension of steel specimens on the change of residual stress rearrangement in a crack domain is investigated experimentally and analytically. Reloading can lead to appearance of residual compressive stress in a crack tip, reduce stress concentration and the probability of crack opening when tensile stress is applied. The stress intensity factor calculation should take into consideration the wide stress range in a crack tip, resulting from its deformation pre-history.

1. Introduction

In most objects, like pressure vessels or pipes, crack is classified as unacceptable defect, especially under dynamic and cyclic loads [1,2]. Numerous methods of Non Destructive Evaluation (NDE): ultrasonic, magnetic, X-ray, eddy current, capillary, and others have as their ultimate objective the detection and localization of a crack. The excluding attitude to a crack is caused by its reduced ability to withstand propagation in the material under the impact of material tensile loading due to strong stress concentration in its tip [3,4]. This ability is quantitatively estimated by the value of the Stress Intensity Factor, which characterizes material fracture strength and which varies for different crack locations in a material relatively to applied load [5]. The reasons for a crack appearance can be fatigue, stress-corrosion, applied stress, exceeding tensile strength of the material, creep, thermal deformations, etc.

To eliminate a sharp decline in the limit of the fracture strength properties of structural materials in the presence of a crack, many theoretical and technological approaches are developed, most of them being focused on the reduction of stress concentration in the tip under crack tension. Among them are vibration, ultrasonic treatment, drilling of holes in the tip, low-temperature annealing, various types of crack traps, and also the so called «autofrettage» technology for thick-walled tubes [6, pp.326-331, 2, pp.970-974, 6.7].

The "autofrettage" technology is commonly used to increase the fracture strength of thick-walled cylinders. It was initiated more than a century ago to handle gun barrels [8]. Injecting high internal pressure in the pipe gives rise to elasto-plastic deformation, inhomogeneous in the radial direction. The result - is a decrease in hoop stress value in the direction from the inner to the outer diameter. Upon reaching the Mises-Henke yield criterion on the inner diameter, a further increase in pressure yields extending plastic flow zone in the direction to the outer surface of the tube. The plastic deformation on inner layers of a tube initiates the new hoop stress distribution pattern, which appears after the relief of the internal pressure: the elastic shrinking of the outer layers yields appearance of compressive residual hoop stress in the internal layers and increase of fracture strength of the pipe. Quantitative characteristics of the operating mode to optimize this hardening process are well known [6-8], but its use is limited to the thick-walled cylinders.

On the contrary, the effect of pre-loading on the stress distribution in thin-walled cylinders, shells and plates, especially in the presence of a crack, is not clear. Compressive stress, arising in the internal layers after elastic-plastic tension and load removal of thin-walled tubes, although positive, are small in value and can not significantly affect the increase of strength properties and reduction of tube fracture strength when subjected to workload. As some NDE techniques (e.g., micro magnetic) recognize crack by its stress pattern, it is interesting, how does a residual stress pattern in a crack domain depends upon the deformation history, and whether is it possible to enhance hardening effect in thin-walled objects, like plates and shells. This paper presents the results of the experimental and analytical study of this effect, namely change in residual stress distribution pattern in a crack after repeating elasto-plastic tension of steel plates.

2. Samples and experimental technique

To study the metal behavior in the region of a crack in the laboratory, two samples of low-carbon steel S345k with dimensions 200x30mm, *t=5,5mm* were prepared, each having on the surface one unilateral closed micro crack with the crack-tip opening displacement of 3 μk (sample 1) and 5 μk (sample 2), the radius of curvature at the crack tips were 1.5 μk and 2.5 μk respectively, the depth of about *b=0,9* mm and length *2a* respectively 16 and 18 mm (fig.1, top). The cracks were obtained by the original technology of electro-chemical treatment. In the sample 2, before testing, the hole at one edge of the crack was drilled with a diameter of 1 mm and depth of 2 mm to remove the sharp stress concentrator in the tip. Arrangement of strain gages on the samples is shown in Figure 1, bottom.

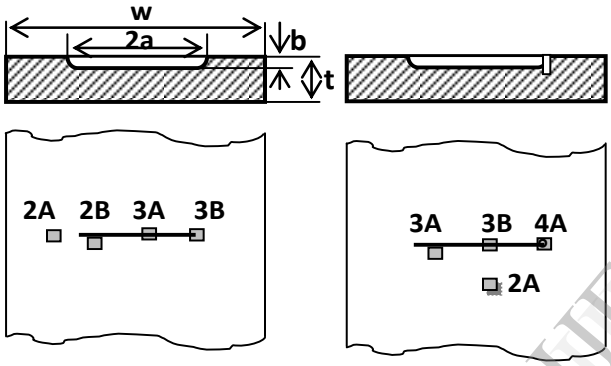

Figure 1. Specimens (1 - left, 2 - right) with surface microcracks having crack-tip opening displacement 3 and 5 μk respectively. The crack in the specimen 2 had drilled closed hole in the tip with 1 mm diameter and 2 mm depth. Crack parameters are shown in the right top picture. The strain gages locations on both surfaces are shown in the lower pictures

Cracks were identified by a dye penetrant flaw detection. The chemical composition of the steel, the yield strength, σ_y, and tensile strength, σ_d, are shown in the Table 1.

Table 1. Chemical composition of steel S345k and strength characteristics

C	Si	Mn	Ni	S	P
to 0.12	0.17 - 0.37	0.3 - 0.6	0.3 - 0.6	to 0.04	0.07 - 0.12
Cr	N	Al	Cu	σ_y	σ_d
0.5 - 0.8	to 0.012	0.08 - 0.15	0.3 - 0.5	345 MPa	470 MPa

Other crack parameters are: b = 0,9 mm, $\alpha = b/a$, $\beta = b/t$. For those values of α and β [9, par. 1.16] the ultimate stress intensity factors at points A and B were, respectively, $K_{1,C}$=*1770,8 кг/см*$^{3/2}$, $K_{1,D}$=*806,7 кг/см*$^{3/2}$ for the first specimen with the crack, and $K_{1,C}$=*1788,8 кг/см*$^{3/2}$, $K_{1,D}$=*773,3 кг/см*$^{3/2}$ – for the second.

In the experiments, using the machine Instron, samples were loaded by tension and unloaded after each loading repeatably. Gage outputs were connected to the input of originally developed precision multi-functional multi-channel strain gage station and special software, enabled serial (with 1 sec period) records from strain gages with 1 mm base, glued over the crack and to basic metal respectively.

Figure 2 shows the results of measuring strain values in the crack under repeated loading-unloading of the sample 1 below or above the yield stress value (in each loading cycle respectively). Figure 3 shows the loading-unloading diagrams - the stress-strain dependence (stress is calculated as the ratio of load to sample's full cross section) in a crack domain of the sample 1. Figure 4 shows strain values variation in a crack domain under loading-unloading of the sample 2 before break (in the 3rd loading cycle). Figure 5 shows stress-strain diagrams of metal under repeated loading-unloading of the sample 2. Figure 6 shows the photo of the cross section of the sample 2 after the damage, where the crack surface is visible at the top part.

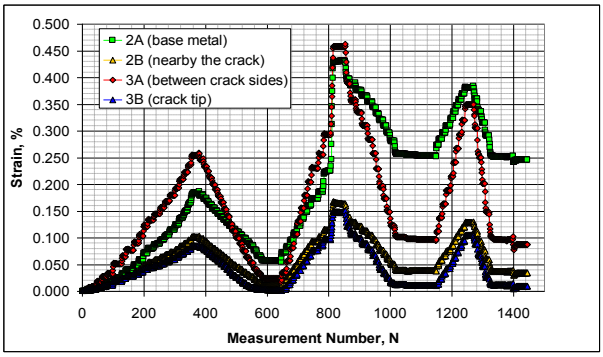

Figure 2. Serial records from strain gages placed in the surface spots, shown in the fig.1. Three cycles of tension loading-unloading were done before the specimen 1 failed

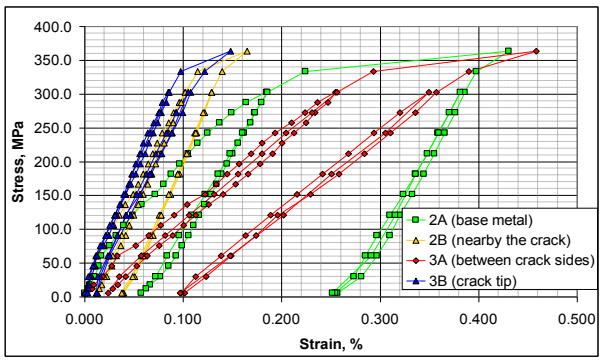

Figure 3. Stress-strain diagrams of the metal in surface spots, shown in the fig.1. Three cycles of tension loading-unloading were done before the specimen 1 failed

3. Experimental results

Figures 2,4 provide information on the strain kinetics, while Figures 3,5 show stress-strain behavior in different points of the sample, deformed by tension repeatedly in the elastic-plastic domain. As stated, the samples 1 and 2, in principle, differ in that, in the first - the crack is in its natural state in the tip, and in the second - the unloading hole 0.5 mm radius is drilled in the crack tip. As shown in Figures 2-5, the deformation features in different zones are in principal differ.

Sample 1 (Fig. 2 and Fig. 3): 3 cycles of quasi-static loading. In the first cycle the base metal (green diagram 2A) is loaded to the yield point (ε ~ 0,2%), which corresponds to the absolute elongation of ~ 2.0×10^{-3} mm on the base 1mm. While loading the crack-tip opening displacement (red) advances the elongation of the base metal, the absolute elongation on the 1 mm base being larger and equal to 2.5×10^{-3} mm. The crack and base metal strain compatibility is ensured by the fact that the excess of the crack opening (red 3A) is compensated by the decrease in deformation of the metal near the crack (yellow 2B), the absolute value of the latter is less than ~ 1.0×10^{-3} mm. Absolute strain at the crack tip (blue 3B) is difficult to estimate quantitatively because of the extreme heterogeneity of its distribution in the 1mm strain gage installation zone. Nevertheless, due to the strain compatibility condition, it is clear that within the narrow region in the crack tip the plasticity occurs (see the simulation results in different deformation zones in the next section) to ensure the large widening of the crack in the central zone.

Slow unloading of the sample yields appearance, in the end of the first cycle, of the residual strain which differs in different zones (Fig. 2,3). When unloading, the crack closure rate (Figure 2, the slope of the red 3A unloading diagram) is significantly higher than the rate of the base metal shrinkage (green 2A) outside the crack; at some point (ε ~ 0,12%) strains are aligned, then in the base metal, according to the equilibrium condition, the residual tensile strain (and stress), while in the cracks – compression strain (and stress) occur. (It is clear that the main reason of this effect is the inhomogeneity of the elastic-plastic deformation in different parts of the sample under load). The residual compressive strain value can be estimated very roughly by examining the correlation of the residual strain in different zones (Fig. 3). Residual strain at the crack tip after the first cycle is zero (blue 3B), or even negative, and the crack strain ~0.02% (red 3A) is lower than the strain value of the base metal (green 2A). It is clear that the difference between these strains (~0.04%) acts as a pressure, compressing the crack. Roughly one can estimate its value equal $\sigma = E\varepsilon = 2{,}1 \cdot 10^5 \cdot 4 \cdot 10^{-4} \approx 80$ MPa. Eligibility of the above assessment of stress value, arising in the crack, is reasonable only being applied to the sample type, used in the experiment, in which the crack length is half of the width of the sample. The smaller is the crack length and larger is the plastic zone area, the stronger will be the effect of compression, or "hardening" of the crack.

In the second cycle the maximum strain in the base metal was increased to ε ~ 0,45% (Figure 4) and was accompanied by a pronounced plastic flow (Fig. 5). When unloading the described effect of residual compressive strain appearance in the base metal has become more intense, the residual strain in the crack tip slightly increased to about 0.01% (blue), the strain value in the base metal (green) - 0.25%, and the strain value in the crack (red) - 0.1%. The compressive pressure exerted by the base metal on the crack, is, therefore, 0.15%, and the corresponding compressive stress - about 300 MPa. The residual compressive strain in the crack tip contributes to the growth of a critical K_1-value providing a kind of crack "hardening" effect. Thus, the growing positive difference between the residual strain values of base metal and crack respectively contributes to the crack hardening effect. The possibility appears to apply in practice the effect of crack "hardening" under repeated loading, a kind of «crack-train» mode.

However, in the third loading-unloading stage the effect of "hardening" was not observed any more despite of the significant absolute value of the base metal strain value under load. In our opinion, this is due to the previous crack "hardening" stage and the delay, for this reason, of the plastic flow beginning in the crack tip (as is seen in Fig. 5, it does not arise at all.)

Hardening effect is also influences the magnitude of fracture stress value, which, as can be seen by comparing Figure 3 and Figure 5 for two sample types, is approximately the same in spite of the elimination of stress concentrator in the sample 2.

Sample 2 (Figure 4 and Figure 5): the appearance of the unloading hole at the crack tip (Figure 4 and Figure 5) substantially changes the distribution of strain in the area around the crack. The most significant inelastic behavior is demonstrated by the crack-tip opening displacement (blue figure 3B). Almost at all stages of loading and unloading the crack-tip opening displacement exceeds strain value in the base metal. Strain value in the unloading hole (Figure 4A) and in the base metal (green chart 2A) are aligned and become close to each other, and the crack-tip opening (3B) is increased until the sample damage at the third phase. The unloading hole contributes thus to equalizing of strain values in different zones of the sample and to the minimization of hardening effect. There was also observed a significant difference in strain values in the base metal from both crack and opposite to it sides of the plate (green diagrams 2A and 2B, respectively): from the crack side the strain value leaves always lower. This difference appears as a way to restore strain values compatibility in different parts of the sample.

Figure 6 displays the destroyed cross section of the sample in the crack zone. The enlarged diameter of the drilled hole also indicates the appearance of residual compression strain in the crack tip while approaching to the surface.

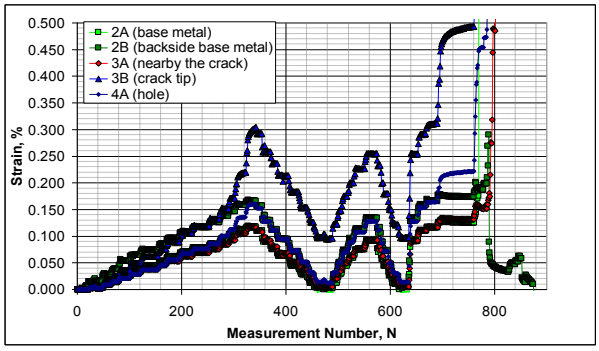

Figure 4. Serial records from strain gages placed in the surface spots, shown in the fig.1(right). Three cycles of tension loading-unloading were done before the specimen 2 failed

4. Numerical simulation

Numerical simulation was carried out using the finite element method (FEM). As a model, the plate with the crack parameters close to the parameters of the samples, used in the experimental study, was investigated. The calculations were performed considering the occurrence of plastic flow in the base metal, the crack and its edges respectively. This involves using Tresc yield condition (III strength theory) or Mises yield condition (IV strength theory).
As the model, the surface crack of 16 mm length, 1 mm depth and 0.1 mm opening, located in the plate with a net section of 40x4 mm, was used. As the stress-strain curve, the extrapolated curve, obtained in the tests with real samples, was used for the simulation (Figure 7).

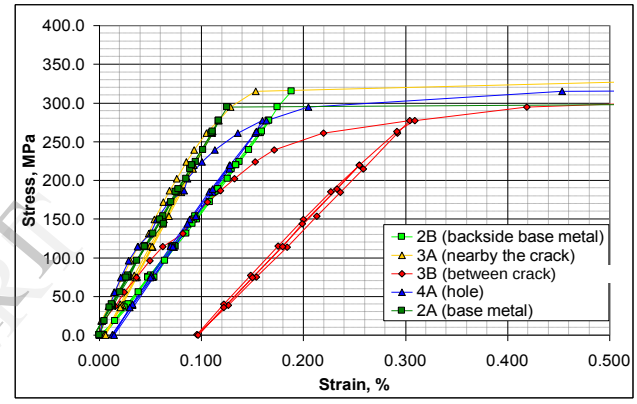

Figure 5. Stress-strain diagrams of the metal in the surface spots, shown in the fig.1. Three cycles of tension loading-unloading were done before the specimen 2 failed

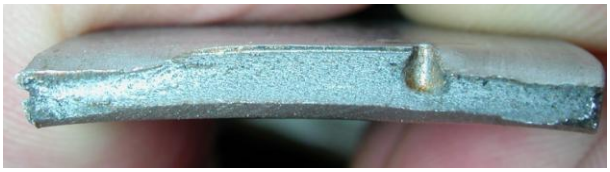

Figure 6. Photo of the sample 2 after the break

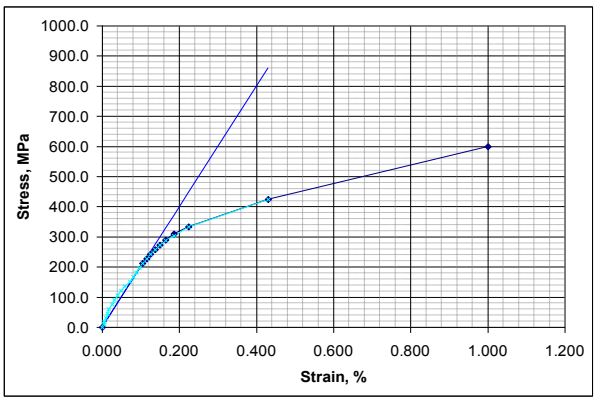

Figure 7. Experimental elastic-plastic stress-strain curve (blue) and extrapolated line (dark blue), both used for the simulation

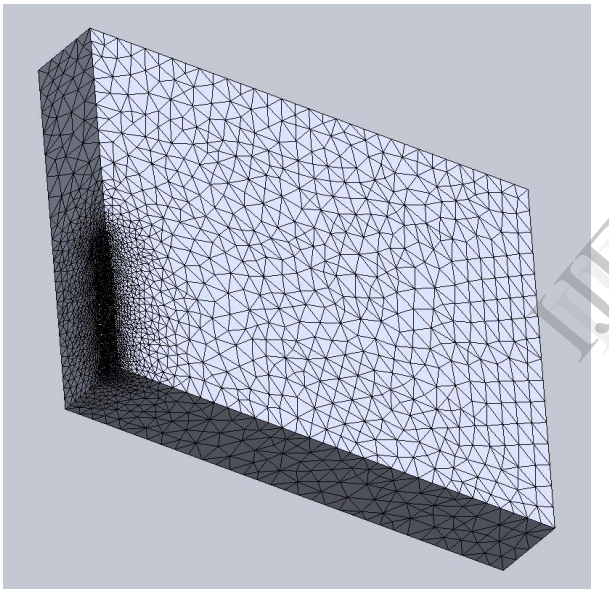

Figure 8. The splitting matrix for the model part (the 1/4 symmetric part of the plate used for calculation)

Figure 8 shows the splitting (finite elements) matrix for the model part (the 1/4 symmetric part of the plate used for calculation). Mean size of the elements is 0.1 mm in the region of the crack and 1 mm - in the rest area. The total number of elements was 49,805, lattice points - 74,587. In calculations the model was "loaded" so that the stress in the defect-free part of the model either corresponded to the stress value of 67% of the yield strength (Tresc condition), or to that of the steel yield strength itself (Mises condition). For selected model these stresses were approximately 200 and 300 MPa respectively.

In the figures 9 the simulation results at two deformation stages in the specimen with a crack are shown. The specific calculated stress distribution in the crack domain under the successive loading up to 200 MPa and the load removal are shown respectively. As can be seen from the figures, when loaded, at the tip and on the edges of cracks there occur the plastic flow zones, which are replaced by residual compressive stress zones after load removal. This is accompanied by the fact, that during unloading the reduction in crack advances deformation reduction of the base metal. Subsequent unloading leads to the fact, that the base metal, to some extent, compresses the crack, creating at its tip the residual compressive stress. The calculation showed that the subsequent loading of up to 200 MPa does not practically changes the stress distribution pattern under load and residual stress pattern as well.

To confirm the eligibility of referring the strain kinetics in the figures 2 and 4 to the appearing of compression zones in the crack tip (as shown in the figure 9) after loading over yield limit value and subsequent unloading, we demonstrate in the figure 10 the simulated stress kinetics in the crack tip, the crack itself and in the defect-free area, which resulted in the patterns shown in the figure 9.

The proposed strain trial of steel pipes to reduce the risk of a crack can be considered as pipe "stress-test" trial.

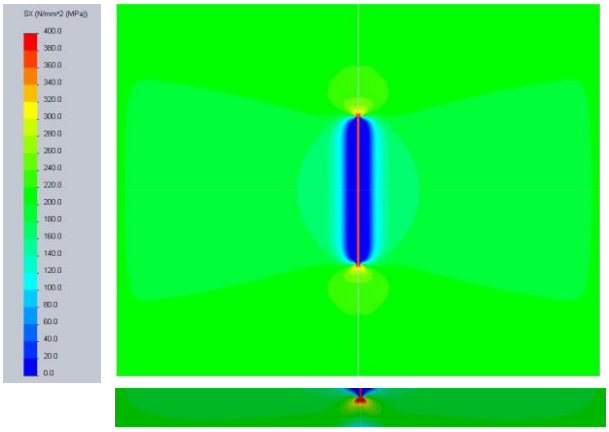

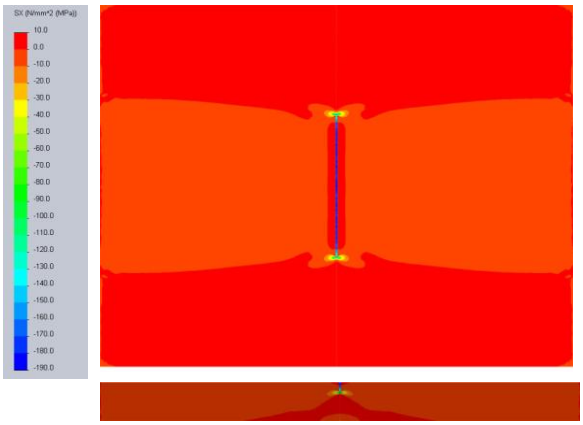

Figure 9. Stress distribution in the crack domain: under loading (top-down - top view, longitudinal cross section); when the load is removed (top-down - top view, longitudinal cross section)

5. Conclusion

1. Experimental trials and computational approach have shown that the repeated loading of the material with one side dead-end crack to a stress value close to the base material yield stress, can result in appearance of the residual compressive stress in the crack tip and the base metal, which can reduce stress concentration in the and thus the probability of crack propagation under applied tension load, a kind of a «crack-train» trial. Optimization of the «crack-train» trial conditions may result in the alignment in the strength of material with a crack and without it respectively.

2. The proposed method of modeling the behavior of the metal in the crack domain can be used for the condition optimization for a «crack-train» test, the most easily implemented within the «stress-test» trial of thin-wall pipes.

3. Usually only one or two cycles of loading under optimal conditions are sufficient to achieve the desired effect of strengthening. Subsequent loading cycles usually, at least, do not enhance this effect.

4. Prior, before the «crack-train» cycle removal of stress concentrator at the “crack tip” by drilling the unloading holes, does not contribute to the subsequent enhance of the "hardening" effect, which is in fact the result of considerable spatial stress heterogeneity in a crack domain under its tensile deformation.

References

[1] Parton V.Z. and Boriskovski V.G. Brittle Fracture Dynamics. Moscow: “Machine Building”, 1988.

[2] Morozov N.F. and Petrov U.V. Problems of Fracture Dynamics of Solids. S.-Petersburg: S.-Petersburg State Un-ty, 1997.

[3] Cherepanov G.P. Brittle Fracture Mechanics. Moscow: Nauka, 1974.

[4] Goldstyne R.V. Plasticity and Fracture of Solids. Moscow: Nauka, 1988.

[5] Antipov B.N. Rehabilitation Technology of Pipelines after Repair. Exposition Oil and Gas. 2009, № 2, pp. 29-31.

[6] Parker A.P. Autofrettage of open-end tubes – pressures, stresses, strains, and code comparisons. Journal of pressure vessel technology, V.123, August 2001, pp.271-277

[7] Majzoobi G.H., Farrahi G.H., Mahmoudi A.H., A finite element simulation and an experimental study of autofrettage for strain hardened thick-walled cylinders, J.Mater. Sci. Eng. A., vol. 359 pp. 326-331, 2003.

[8] G.J. Franklin, JLM. Morrison. Autofrettage of cylinders: prediction of pressure, external expansion curves and calculation of residual stresses. Proceeding of Institute of Mechanical Engineers, vol. 174, pp. 947-974, 1960.

[9] Stress Intensity Factors Handbook. Vol.1,2. Ed.by Y.Murakami. Pergamon Press. 1986.